The Structure of the S127P Mutant of Cytochrome b_5 Reductase that Causes Methemoglobinemia Shows the AMP Moiety of the Flavin Occupying the Substrate Binding Site†

Maria C. Bewley,*,‡,§ C. Ainsley Davis,|| Christopher C. Marohnic,|| David Taormina,‡ and Michael J. Barber||

Biology Department, Brookhaven National Laboratory, Upton, New York 11973, and Department of Biochemistry and Molecular Biology, College of Medicine, University of South Florida, Tampa, Florida 33612

Received May 29, 2003; Revised Manuscript Received September 4, 2003

ABSTRACT: Methemoglobinemia, the first hereditary disease to be identified that involved an enzyme deficiency, has been ascribed to mutations in the enzyme cytochrome b_5 reductase. A variety of defects in either the erythrocytic or microsomal forms of the enzyme have been identified that give rise to the type I or type II variant of the disease, respectively. The positions of the methemoglobinemia-causing mutations are scattered throughout the protein sequence, but the majority of the nontruncated mutants that produce type II symptoms occur close to the flavin adenine dinucleotide (FAD) cofactor binding site. While X-ray structures have been determined for the soluble, flavin-containing diaphorase domains of the rat and pig enzymes, no X-ray or NMR structure has been described for the human enzyme or any of the methemoglobinemia variants. S127P, a mutant that causes type II methemoglobinemia, was the first to be positively identified and have its spectroscopic and kinetic properties characterized that revealed altered nicotinamide adenine dinucleotide hydride (NADH) substrate binding behavior. To understand these changes at a structural level, we have determined the structure of the S127P mutant of rat cytochrome b_5 reductase to 1.8 Å resolution, providing the first structural snapshot of a cytochrome b_5 reductase mutant that causes methemoglobinemia. The high-resolution structure revealed that the adenosine diphosphate (ADP) moiety of the FAD prosthetic group is displaced into the corresponding ADP binding site of the physiological substrate, NADH, thus acting as a substrate inhibitor which is consistent with both the spectroscopic and kinetic data.

Cytochrome b_5 reductase (cb_5r,[1] EC 1.6.2.2), a vital component enzyme of the microsomal electron transport system and erythrocyte function, catalyzes the transfer of reducing equivalents from NADH to two molecules of the small heme-containing protein cytochrome b_5. The enzyme contains a single, tightly bound FAD prosthetic group and exists in two forms, a membrane-bound form (*1*) comprised of both a hydrophobic membrane-anchoring domain ($M_r \sim$ 3 kDa, residues 1−25) and a hydrophilic, catalytic, or diaphorase domain ($M_r \sim$ 30 kDa, residues 26−300) and a soluble, truncated form (*2*) comprising only the catalytic domain. The membrane-bound form of cb_5r is embedded in the membranes (endoplasmic reticulum, mitochondria, and nuclear and plasma membranes) of somatic cells and, together with the membrane-bound form of cb_5, participates in a diverse array of metabolic transformations. These include the desaturation and elongation of fatty acids (*3*, *4*), specific P450-mediated hydroxylation reactions (*5*), and cholesterol biosynthesis (*6*). Specific examples include catalysis by Δ9-, Δ6-, and Δ5-acyl CoA desaturases (*7*), alkyl acyl-glycero-3-phosphoryl ethanolamine desaturase (*8*), phospholipid desaturase (*9*), fatty acid elongation enzyme (*4*), Δ7-sterol Δ9-desaturase (*6*), *N*-hydroxylamine reductase (*9*), 4-methylsterol oxidase (*10*), prostaglandin synthase reductase (*11*), and cytochrome P450 3A4 (*12*).

The soluble form of cb_5r exists in circulating erythrocytes and catalyzes methemoglobin reduction (*13*). This function is critical, since elevated levels of methemoglobin give rise to cellular hypoxia, resulting in death when methemoglobin levels approach 70%. Children, especially those younger than 4 months of age, are particularly susceptible to methemoglobinemia, possibly because the primary erythrocyte protective mechanism against oxidative stress in infants has not

† This work was supported by Department of Energy LDRD Project 00-43 (MCB), Grant GM32696 from the National Institutes of Health (M.J.B.), and Grant 0150936B from the American Heart Association, Florida/Puerto Rico Affiliate (M.J.B.). We extend our thanks to the Department of Energy summer graduate program which provided a stipend for D.T. to gain research experience in the lab of M.C.B.

* To whom correspondence should be addressed: Department of Biochemistry and Molecular Biology, Mail Code H171, Pennsylvania State College of Medicine, 500 University Dr., P.O. Box 850, Hershey, PA 17033-0850. Telephone: (717) 531-4324. E-mail: mcb21@psu.edu.

‡ Brookhaven National Laboratory.

§ Current address: Department of Biochemistry and Molecular Biology, Mail Code H171, Pennsylvania State College of Medicine, 500 University Dr., P.O. Box 850, Hershey, PA 17033-0850.

|| University of South Florida.

[1] Abbreviations: cb_5r, cytochrome b_5 reductase; cb_5, cytochrome b_5; FNR, ferredoxin:$NADP^+$ reductase; NADH:FR, NADH:ferricyanide reductase; NADH:BR, NADH:cytochrome b_5 reductase; SDS, sodium dodecyl sulfate; PAGE, polyacrylamide gel electrophoresis; FPLC, fast protein liquid chromatography; MOPS, 3-(*N*-morpholino)propanesulfonic acid; Tris, tris(hydroxymethyl)aminomethane; PCR, polymerase chain reaction; EDTA, ethylenediaminetetraacetic acid; PMSF, phenylmethanesulfonyl fluoride; TB, Terrific Broth.

10.1021/bi034915c CCC: $25.00
Published on Web 10/24/2003

fully matured, and the cb_5r activity and concentrations are low.

Defects in cb$_5$r have been identified as the major cause of recessive congenital methemoglobinemia (RCM, MIM 250800) (*14*), the first example of a hereditary disease associated with a specific enzyme deficiency (*15*). Several mutations of the human gene encoding cb$_5$r have been shown to result in either the type I or type II form of methemoglobinemia (*14*, *16*, *17*). The type I disease results from a deficiency in cb$_5$r activity in circulating erythrocytes, causing clinical symptoms of cyanosis (*18*), whereas the more severe type II disease results from loss of both the membrane-associated and soluble forms of cb$_5$r, causing both cyanosis and impaired fatty acid biosynthesis, with patients often suffering premature death from severe developmental abnormalities (*19*).

The first RCM mutant to be genetically identified was from a patient with the type II, generalized disease. A single T → C transition was identified at the initial position of codon 127 in exon 5 of the DIA1 gene, resulting in replacement of a serine residue with proline (*20*). Spectral and kinetic analyses of a recombinant form of the S127P[2] mutant indicated alterations in the spectral properties of the FAD prosthetic group together with decreased catalytic activity (*21*). These results were interpreted in terms of S127 functioning in a critical role in maintaining the structure of the NADH binding site.

To understand the structural perturbations caused by the S → P substitution at the atomic level, we have determined the X-ray structure of a recombinant form of the rat cb$_5$r S127P variant at 1.8 Å resolution. The structure indicates that substitution of proline for serine at residue 127 predominantly results in an altered FAD conformation in which the flavin ADP moiety occupies part of the substrate (NADH) binding site, reducing enzyme efficiency.

MATERIALS AND METHODS

Materials. NADH, NAD$^+$, 5′-ADP-ribose, 5′-ADP, AMP, riboflavin, PMSF, and Tris base were purchased from Sigma Chemical Co. (St. Louis, MO). MOPS was purchased from Calbiochem (San Diego, CA). Native *Pfu* and *Pfu* Turbo polymerases as well as the *Escherichia coli* BL21-CodonPlus (DE3)-RIL cells were obtained from Stratagene (La Jolla, CA). The restriction enzyme *Alw*NI was obtained from New England Biolabs (Beverley, MA). Triton X-100 and Hot Start Micro 50 PCR tubes were obtained from Molecular-Bio Products Inc. (San Diego, CA). IPTG was obtained from RPI (Mt. Prospect, IL), while tryptone and yeast extract were obtained from EM Science (Gibbstown, NJ). Ni−NTA agarose and kits for plasmid preparation and agarose gel extraction were purchased from Qiagen Inc. (Valencia, CA). Nucleotide sequencing was performed by the Molecular Biology Core Facility of the H. Lee Moffitt Cancer Center and Research Institute at the University of South Florida.

Site-Directed Mutagenesis, Protein Expression, and Purification. Site-directed mutagenesis of the pH4CB5R construct to replace S127 with a proline residue was performed in a manner analogous to that described previously (*22*). Two oligonucleotides, corresponding to 5′-CCAGCTGGAGGGAAAATGCCGCAATACCTGGAAAAC-3′ and its complement, were utilized in a PCR that resulted in the required S127P amino acid substitution together with a silent mutation that added an extra *Alw*NI restriction site to facilitate mutant screening. Both the wild type and the S127P variant of the soluble, flavin domain of rat cb$_5$r were efficiently expressed in *E. coli* BL21-CodonPlus (DE3)-RIL cells and purified to homogeneity, as indicated by a single protein band following SDS−PAGE analysis, described previously (*22*). The soluble form of rat cytochrome b_5 was isolated as described by Beck-von Bodman *et al.* (*23*).

Spectroscopy. UV−visible absorption spectra were obtained using a Hewlett-Packard (Agilent Technologies, Palo Alto, CA) 8453 diode-array spectrophotometer. UV and visible CD spectra were obtained using a JASCO (Easton, MD) J710 spectropolarimeter as previously described (*24*). Dissociation constants for complexes of both wild-type cb5r and the S127P variant with 5′-ADP-ribose were determined by differential spectroscopy using a Shimadzu (Columbia, MD) UV-2501PC spectrophotometer (*25*). Oxidized enzyme at concentrations of approximately 50 μM was titrated with increasing concentrations of 5′-ADP-ribose at 25 °C in 3 mM potassium phosphate buffer containing 0.1 mM EDTA at pH 7.0. The K_d was determined by fitting the resulting difference data to the theoretical equations for a 1:1 binding model.

Enzyme Activity. Initial rate kinetic constants for both NADH:FR and NADH:BR activities under conditions of constant pH and ionic strength were determined in 116 mM MOPS buffer, containing 0.1 mM EDTA (pH 7.0, $\mu = 0.05$) as previously described by Marohnic and Barber (*22*).

Crystallography. Crystals were grown by the sitting drop method. Two microliters of protein solution and 2 μL of reservoir were mixed over a reservoir of 500 μL of precipitant. The reservoir contained 12% glycerol and 1.5 M ammonium sulfate in 100 mM Tris buffer at pH 8.5. Crystals grew as orthorhombic prisms over the period of a few days. A complete data set was collected from a single crystal on beamline X12B at the National Synchrotron Light Source at the Brookhaven National Laboratory using standard techniques (*26*). The S127P crystal grew in monoclinic space group $P2_1$, with the following unit cell dimensions: $a = 77.23$ Å, $b = 48.00$ Å, $c = 77.25$ Å, and $\beta = 107.7°$. It contained two molecules in the asymmetric unit and had an estimated solvent content of 45% (*27*). The structure was determined by molecular replacement in Amore (*28*) using the protein coordinates of rat cb$_5$r (*26*). All refinement steps used the program CNS (*29*). The model was subject to rigid body refinement. The coordinates for S127 and atoms within a 5 Å sphere were omitted from the subsequent refinement. A cycle of simulated annealing at 3000 K and individual isotropic temperature refinement were performed prior to initial map calculation. The model was fitted to the map, and the FAD molecule was built into the density. Further refinement, punctuated by rounds of model building, was performed until the model could not be improved as judged by a reduction in R_{free}. The final refinement statistics are summarized in Table 1. Coordinates for the S127P variant of cb$_5$r have been deposited in the Protein Data Bank as entry 1QX4.

[2] Residues are numbered with respect to their position in the full-length, membrane-associated form of cytochrome b_5 reductase.

Table 1: Data Collection and Structure Refinement Statistics for the Rat cb_5r S127P Mutant[a]

data collection	
resolution range (Å)	35.0−1.8
no. of reflections	48325
R_{merge}[b] (%)	6.4 (8.3)
completeness (%)	96.0 (74.8)
redundancy	3.6 (2.8)
$I/\sigma(I)$	23.6 (9.3)
structure refinement	
resolution range (Å)	30.0−1.8
no. of reflections	48320
R_{factor} (%)	20.7
R_{free} (%)	24.1
no. of reflections in the free set	1014
no. of protein atoms	4226
no. of FAD atoms	106
no. of water molecules	256
rmsd for bond lengths (Å)	0.010
rmsd for bond angles (deg)	1.4

[a] Numbers in parentheses refer to data in the outermost resolution shell. [b] $R_{merge} = \sum|I_{ibs} - I_{avg}/\sum I_{avg}$.

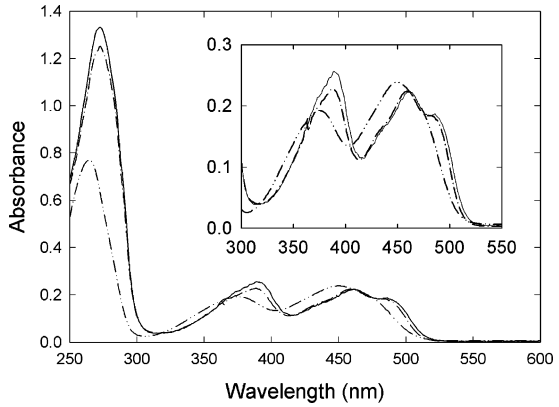

FIGURE 1: Comparison of the UV−visible spectra obtained for the S127P and wild-type forms of rat cytochrome b_5 reductase. UV−visible spectra were obtained for the oxidized forms of S127P (−·−) and wild-type (−) rat cb_5r (2 μM FAD) in 10 mM potassium phosphate buffer containing 0.1 mM EDTA (pH 7.0). The spectrum obtained from a sample of free FAD (2 μM, −··−) in 10 mM potassium phosphate buffer containing 0.1 mM EDTA (pH 7.0) is shown for purposes of comparison. The inset shows the flavin absorbance on an expanded scale.

RESULTS AND DISCUSSION

Spectroscopic and Kinetic Properties of the S127P Variant. To confirm that the S127P variant of rat cb_5r retained the spectroscopic and kinetic properties characteristic of the corresponding human mutant, both UV−visible absorbance and CD spectra were obtained together with NADH:FR and NADH:BR activity measurements.

Comparison of the UV−visible absorbance spectra obtained for the purified wild-type and S127P forms of cb_5r, shown in Figure 1, indicated that in the mutant protein, absorbance maxima corresponding to the FAD prosthetic group were blue-shifted when compared to those of the wild-type enzyme. In the wild-type domain, absorbance maxima were observed at 276, 389, and 461 nm together with the characteristic shoulder at 485 nm. In contrast, while the S127P variant retained the UV maximum at 276 nm, in the visible region, the maxima were shifted to 388 and 458 nm, respectively, together with a small reduction in the definition of the latter peak's shoulder, in agreement with results previously obtained for the human S127P mutant (*21*).

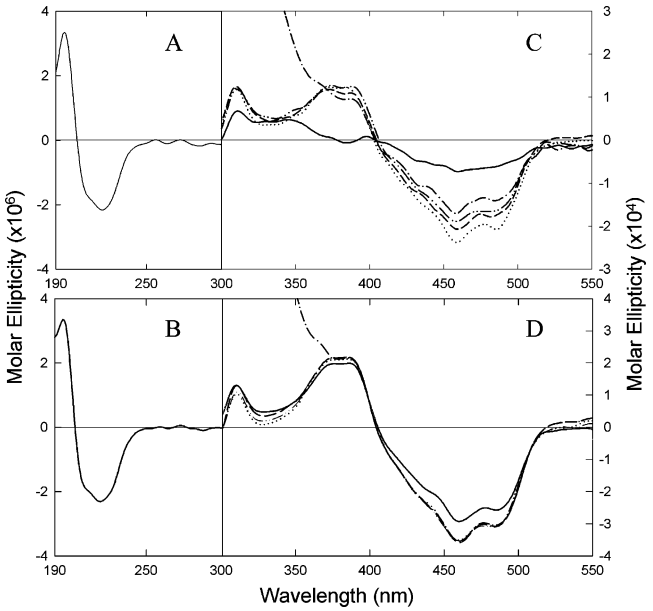

FIGURE 2: Comparison of the UV and visible CD spectra obtained for the S127P and wild-type forms of rat cytochrome b_5 reductase. UV CD spectra were obtained for the S127P (A) and wild-type (B) forms of cb_5r (4 μM FAD) in 10 mM potassium phosphate buffer containing 0.1 mM EDTA (pH 7.0) as previously described (*22*). Visible CD spectra were obtained for the S127P (C, −) and wild-type (D, −) cb_5r (60 μM FAD) in 10 mM potassium phosphate buffer containing 0.1 mM EDTA (pH 7.0). Spectra were also obtained for the S127P and wild-type cb_5r in the presence of 15 mM NAD^+ (−·−), 10.4 mM 5′-ADP-ribose (−··−), 12.6 mM 5′-ADP (···), and 14.9 mM AMP (- - -).

In contrast to the visible absorbance spectra, the visible CD spectrum of the S127P mutant revealed a more dramatic change when compared to that of the wild-type cb_5r spectrum. As shown in Figure 2A, in the UV region, the CD spectrum of the S127P variant showed very little change in either the line shape or intensity of the spectrum when compared to that of the wild-type enzyme (Figure 2B), an indication of the absence of any substantial alterations in the overall architecture of the α-helix or β-sheet structural components when compared to the wild-type domain. However, for the visible CD spectrum, substantial changes in the intensities of the various CD transitions were observed. In the oxidized state, the S127P variant exhibited a CD spectrum (Figure 2C) that was markedly diminished in intensity from that of the wild-type protein (Figure 2D) while still retaining weak positive and negative transitions at approximately 390 and 460 nm, respectively, indicating a substantial perturbation of the flavin structure.

The structural changes indicated from the CD spectra of the S127P mutant were also reflected in changes in the catalytic properties of the enzyme. Alterations in the initial rate kinetic parameters obtained for the S127P mutant, when compared to those of wild-type cb_5r, are shown in Table 2. At pH 7, k_{cat} for the NADH:FR activity of the S127P variant was 300 s^{-1}, corresponding to approximately 38% of wild-type activity (k_{cat} = 800 s^{-1}), while the K_m^{NADH} increased more than 9-fold, from 6 to 55 μM. Similarly, for the NADH:BR activity, k_{cat} for the S127P mutant was reduced to approximately 30% of the wild-type value together with a nearly 9-fold increase in the K_m for NADH. However, the K_m values obtained for cb_5 for the mutant and wild-type enzyme were equivalent. These results indicated that both

Table 2: Comparison of the Kinetic Constants Obtained for the Cytochrome b_5 Reductase S127P Mutant and Wild-Type Enzyme

	NADH:FR				NADH:BR			
protein	k_{cat} (s^{-1})	K_m^{NADH} (μM)	K_m^{FeCN} (μM)	k_{cat}/K_m^{NADH} (s^{-1} M^{-1})	k_{cat} (s^{-1})	K_m^{NADH} (μM)	K_m^{cytb5} (μM)	k_{cat}/K_m (s^{-1} M^{-1})
S127P	300 ± 35	55 ± 4	8 ± 1	5.45×10^6	106 ± 17	25 ± 3	14 ± 2	4.24×10^6
wild type	800 ± 33	6.0 ± 0.4	7 ± 1	1.33×10^8	367 ± 20	3.0 ± 0.2	13 ± 3	1.22×10^8

Table 3: Dissociation Constants Obtained for the cb_5r S127P Variant with Various Pyridine Nucleotides

	K_d (mM)	
nucleotide	S127P	wild type
NAD^+	5.0 ± 1.5	0.80 ± 0.01
5′-ADP-ribose	1.5 ± 0.2	0.10 ± 0.01
5′-ADP	0.5 ± 0.1	0.10 ± 0.02
AMP	1.3 ± 0.1	0.80 ± 0.1

the turnover of the enzyme and affinity for NADH were compromised in the mutant, whereas the affinity for cb5 remained unchanged. Further, comparison of the ratios of the specificity constants (k_{cat}/K_m^{NADH}) obtained for the NADH:BR values of the wild type and S127P variants of the rat and human (*21*) enzymes revealed that for both the rat and human enzymes, the S127P mutants retained only 3.5 and 3% of the wild-type values, respectively. These results confirmed that the S127P mutation in rat cb_5r had the same effects on catalytic activity as those previously published for the mutation in the human enzyme.

Dissociation constants obtained for both S127P and wild-type cb5r with a variety of pyridine nucleotides are shown in Table 3. Elevated K_d values were obtained for all the substrate analogues and the S127P mutant. For example, the K_d value for 5′-ADP-ribose for the S127P mutant (1.5 mM) was 15-fold higher than that for the wild-type enzyme (0.1 mM), also suggesting that the mode of binding of this substrate analogue is somewhat altered. This is consistent with previous thermostability studies of the human enzyme that revealed NADH provided only limited protection against inactivation for S127P (*21*).

S127P X-ray Structure. The three-dimensional structure of the flavin domain of the S127P mutant of rat cb_5r was determined at 1.8 Å resolution. The final model contained two copies of amino acid residues T34−F300, two FAD molecules, and 256 water molecules (see Table 1 for data collection statistics). Analysis of the structure indicated that the overall protein fold was similar to that of the wild-type protein, which has been previously described in detail (*26*), and is the classical two-domain arrangement (Figure 3A). Briefly, the structure comprises an amino-terminal FAD binding lobe that comprised residues T34−L147 and a carboxyl-terminal NADH binding lobe corresponding to residues V171−F300. These lobes were linked by a small three-stranded antiparallel β-sheet, comprising residues L148−T170, that has been proposed to act as a "hinge" to orient the two subdomains for efficient transfer of the reducing equivalents from bound NADH to the FAD cofactor in the wild-type enzyme (*26*).

The structure of the S127P mutant showed no significant deviations in the fold compared to the wild-type protein, as shown by low root-mean-square deviations (<0.5 Å for Cα atoms excluding the loop of residues Y112−K125). The main differences in protein structure are concentrated in the loop that is comprised of amino acid residues Y112−K125, which will be termed the "lid". In the native structure, this is a surface-exposed loop that is involved in binding the AMP moiety of the flavin cofactor and will be discussed below in the context of the active site. The lid changes conformation and is displaced ~6 Å relative to the structure of the wild-type enzyme. Despite the movement of the lid in the S127P mutant, the positions of the side chain atoms of K125 remain unchanged compared to the structure of the wild-type enzyme. This residue, as well as K41 and K163, is involved in the formation of active site charge pairs with carboxylate residues of cytochrome b_5 (*30*), and their unchanged positions in the structures of S127P and wild-type cb_5r are in agreement with the biochemical data showing that the S127P mutant of cb_5r retains the same kinetics of cb_5 binding as the wild-type enzyme (Table 2).

The most striking difference between the wild-type and S127P variant structures was observed in the FAD binding site. The initial electron density maps showed clear density for the entire FAD prosthetic group (Figure 3B). In both copies, the conformation of the FAD was identical, but different from that of the wild-type protein.

In the wild-type enzyme, the FAD prosthetic group was located between the two subdomains, but primarily made interactions with the FAD binding lobe. The flavin ADP moiety made extensive interactions with residues in the lid (residues Y112−K125) forming a hydrophobic pocket that housed the adenine moiety, specifically between the planar rings of Y112 and F120. The Oγ atom of S127 was within hydrogen bonding distance of the amide nitrogen atom of Y112 and may assist in stabilizing this loop conformation. The pyrophosphate atoms were accommodated partially by interactions with the Nϵ1 and Nη2 atoms of R91, and the backbone nitrogen atoms of residues G124−S127. The amide nitrogen atom of G124 formed a hydrogen bond with the carbonyl oxygen atom of Y112. The flavin isoalloxazine ring bridged the FAD binding and NADH binding subdomains and was seated in a predominantly hydrophobic pocket, making van der Waals interactions with the side chains of residues R91−T94 in the Fβ4 strand and residues T181−P185 in helix Nα1. These residues are generally conserved and form part of the FAD pyridine nucleotide binding sequence signature, "GxGxxP", in the ferredoxin:$NADP^+$ reductase family of flavoprotein oxidoreductases (*31*).

In the structure of S127P, there was a major conformational change in the lid that may be partially due to the removal of the interaction of the side chain of S127 with the amide nitrogen atom of Y112. A further effect of this mutation was a change in the conformation of G124. The carbonyl oxygen atom of G124 forms a hydrogen bond with the amide nitrogen atom of Q128, resulting in an extension of the Nα1 helix and a displacement of the lid by ~6 Å. This conformational change in the lid obliterates the adenine binding pocket and obscures the pyrophosphate binding site

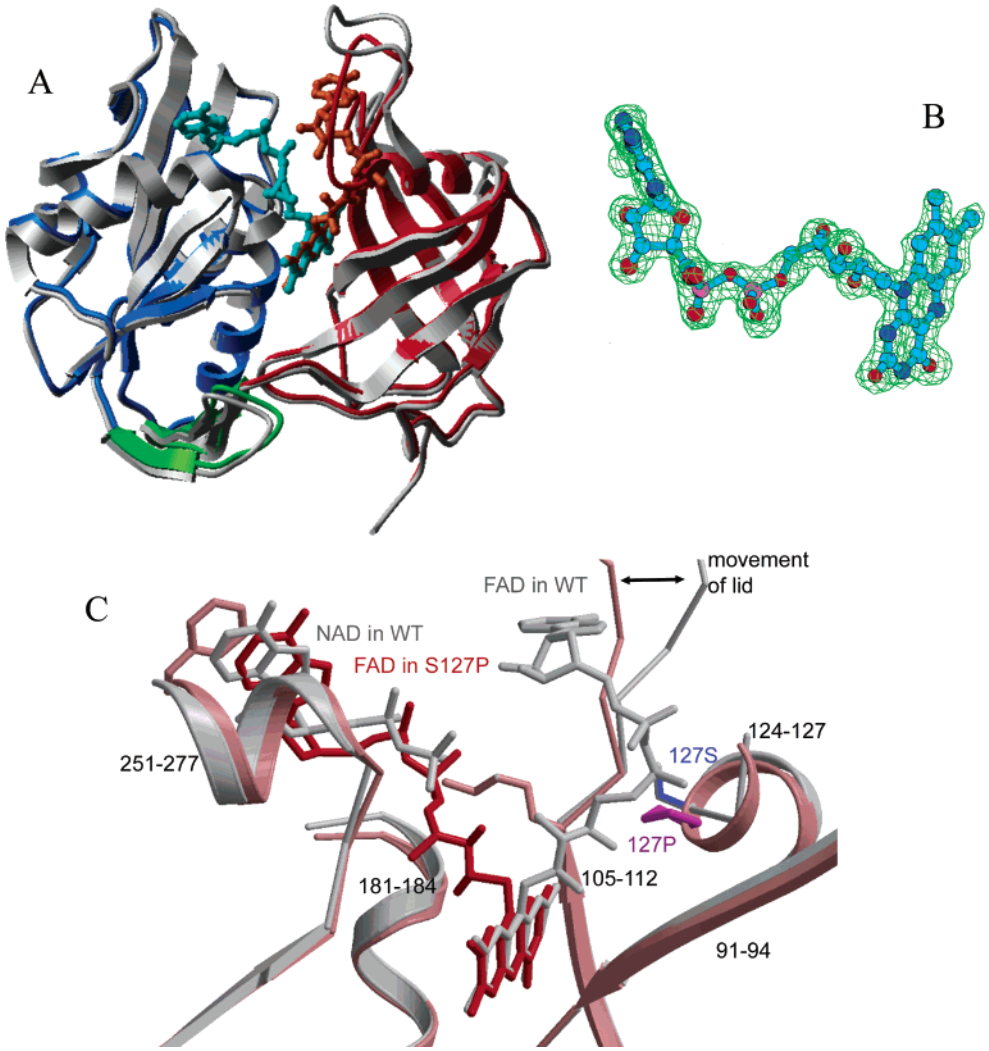

FIGURE 3: Comparison of the FAD environment in the structures of S127P and wild-type rat cytochrome b_5 reductase. (A) Ribbon diagram of the structures of the rat cb_5r S127P and wild-type proteins. The S127P subdomains are colored blue for the NADH and red for the FAD binding domains, while the "linker" region is shown in green. The native structure is shown in gray. The FAD prosthetic group is displayed in a ball-and-stick representation. It is colored cyan in the S127P mutant and orange in the wild-type structures. The movement of the lid is highlighted. (B) The $2F_o - F_c$ electron density of FAD in the structure of the S127P variant. (C) Close-up view of the FAD binding site in the S127P mutant. The structure of the wild type and S127P mutant are colored white and pink, respectively. The positions of residue 127 are highlighted in blue and magenta for the wild type and mutant, respectively. This figure was produced using a combination of Molscript, Bobscript (*40*), and Raster3D (*41*).

of the FAD cofactor. Thus, the position of the flavin ADP moiety is significantly different (Figure 3C) with an ~12 Å displacement of the adenine moiety of the FAD, leaving only the lumiflavin moiety in a similar position, relative to the wild-type protein.

In contrast to the structure of the wild-type enzyme, in the S127P variant, the majority of the interactions of the ADP moiety reside on the previously characterized NADH binding subdomain. The charge on the pyrophosphate group is neutralized by interactions with the Nζ atom of K110, which has previously been shown to be important in substrate binding (*26*, *32*−*34*). The adenine moiety is housed in a 6 Å wide channel formed by residues P275−M277 in the Nα4 helix on one side and F251 on the other. These residues are generally conserved in the FNR superfamily and form part of a second NADH binding sequence signature, "CGPxxM" (*31*). Thus, the ADP moiety of the FAD occupies the ADP binding site of the reducing substrate in the wild-type enzyme (Figure 3C).

Comparison of the X-ray structure obtained for the S127P variant and the visible CD spectra obtained for the mutant and wild-type enzymes indicated that the altered FAD conformation observed in the S127P X-ray structure was also maintained in solution. The major changes observed in the S127P visible CD spectra were confined to alterations in the intensities of the various CD transitions with little change in the apparent peak positions or their polarity. The wild-type visible CD spectrum is well-understood and is characteristic of the coupling of the transition dipoles of the flavin rings; flavin dipoles are oriented approximately from C7 to N1 for the low-energy visible transition (λ_{max} > 450 nm) and from C8 to N3 for the higher-energy transition (λ_{max} > 370 nm) (*35*). Further, a structural change in the ribityl moiety has been previously shown to affect the CD spectrum (*36*, *37*). In the S127P mutant, the peaks were in similar positions with the same polarities when compared to those of the wild-type enzyme, but the intensities of the various transitions were significantly diminished. Since the confor-

mational change in the FAD results primarily from a rotation around the ribityl N10−C1* bond, the observed spectral changes in the CD remain consistent with the hypothesis that the FAD also adopts an altered conformation in the S127P mutant in solution.

In addition, comparison of the initial rate kinetic constants obtained for both the NADH:FR and NADH:BR activities of the wild-type and S127P mutant protein, respectively, suggested that the altered flavin conformation is present in solution. As anticipated from the X-ray structures, the K_m for NADH in the S127P mutant was increased nearly 10-fold for both the NADH:FR and NADH:BR activities with respect to that of the wild-type enzyme. In addition, the k_{cat} for the S127P mutant was also reduced approximately 3-fold. However, the K_m for cytochrome b_5 remained unchanged and in close agreement with the corresponding values previously reported for the purified human wild-type and mutant proteins (*21*), indicating that the mutations had no adverse effect on cb_5 binding. It should also be noted that the reduction in the S127P NADH:BR activity is consistent with the results obtained from the original study of the patient with RCM (*20*).

Application of the crystallographic results obtained for the FAD conformation to the structure of the S127P mutant in solution suggests that the flavin ADP moiety must be displaced during enzyme turnover, since the kinetic data indicated that the electron transfer process, requiring NADH reduction of the enzyme, still operates in the S127P mutant, albeit in a less efficient manner (*21*, *29*). Similar observations have been reported for recombinant variants of porcine cb_5r in which S99 (equivalent to S127 in the rat enzyme) was replaced with alanine, valine, and threonine (*38*). To test this hypothesis, we attempted to soak the substrate analogues 5′-ADP-ribose and NAD^+ into crystals of S127P; however, the crystals cracked, providing additional evidence for a change in the FAD conformation following substrate/product analogue addition. If the crystals were harvested just prior to cracking and data collected, the resultant structures were isomorphous to the structure of the S127P mutant, providing additional evidence that a conformational change in the flavin prosthetic group is required (M. C. Bewley, unpublished data).

While we were unable to examine the potential displacement of the flavin ADP moiety back to its original wild-type position using the S127P crystals, we were able to monitor flavin displacement in solution using CD spectroscopy. To compare flavin displacement in the S127P and wild-type cb_5r, we obtained visible CD spectra for both proteins following the addition of NAD^+ or a variety of pyridine nucleotide analogues. As shown in Figure 2D, addition of these cb_5r product or product analogues to the wild-type protein resulted in no apparent change in the visible CD spectra (Figure 2D), indicating that addition of the pyridine nucleotides had no detectable effect on the conformation of the FAD prosthetic group. However, in contrast, addition of the same compounds to the S127P variant resulted in significant changes in the associated CD spectrum (Figure 2C). In the presence of NAD^+, 5′-ADP-ribose, 5′-ADP, or AMP, the S127P flavin spectrum dramatically increased in intensity, adopting a line shape comparable to that of the wild-type domain. In the presence of the most effective NAD^+ analogue, 5′-ADP, the spectrum for the S127P mutant adopted a line shape and intensity more characteristic of the wild-type enzyme, suggesting that that the ADP moiety of the FAD was being displaced back into its wild-type conformation following the binding of 5′-ADP-ribose. Further, removal of the bound 5′-ADP-ribose by repeated washing of the sample with buffer on a 10 000 molecular weight cutoff membrane resulted in partial reversion of the CD spectrum to one more characteristic of the oxidized S127P mutant, suggesting that the ADP moiety of the cofactor could be reversibly displaced from the NADH binding cleft.

Similar changes in the visible CD spectrum of the S127P mutant were detected during titrations of the protein with 5′-ADP-ribose (results not shown). The CD peak from 350 to 400 nm in the oxidized S127P spectrum became more positive in intensity, while the peaks in the 400−500 nm region became more negative in intensity; on the other hand, the wild-type cb_5r underwent no substantial conformational change in its spectrum during the titration experiment.

The K_d values obtained for the various analogues (Table 3) are also consistent with this displacement hypothesis. Previous studies of the bovine enzyme (*39*) have demonstrated that 5′-ADP-ribose, 5′-ADP, and AMP are more efficient inhibitors of cb5r NADH:FR activity than NAD^+, suggesting that the ADP portion of the pyridine nucleotides was predominantly involved in substrate binding. This trend in analogue affinity was maintained for both the wild type and S127P variants of rat cb5r, although the K_d values for the various analogues were significantly higher for the mutant enzyme than for native cb5r. For the wild-type enzyme, 5′-ADP-ribose and 5′-ADP exhibited equivalent affinities, whereas for the S127P variant, the K_d for 5′-ADP-ribose was 3 times higher than that for 5′-ADP, consistent with the model in which binding of the latter would require less displacement of the FAD prosthetic group.

Thus, the question of why S127P has such a deleterious effect even though it is active when pure recombinant protein is examined remains open. One possibility is that in the cellular environment, its reduced affinity for FAD and NADH has a much greater effect on the catalytic activity than in our optimized *in vitro* reactions. This is consistent with the 10% residual b_5r activity found in lymphoblastoid cells that were homozygous for this mutation (*20*). Alternatively, the mutation may effect an, as yet, unidentified function of b_5r. Integration of the spectroscopic, kinetic, and structural data obtained for the S127P variant of cb_5r suggests that substitution of serine 127 with a proline residue primarily results in a conformational change in the FAD prosthetic group following partial disruption of the cofactor binding site. However, the reducing substrate binding site (NADH) apparently remains unchanged, creating an environment in which the ADP moiety of the FAD can bind. Upon addition of substrate, the ADP moiety of the cofactor can be partially displaced and electron transfer can occur. It is interesting to note that similar spectral changes have been reported for a range of site-directed mutants of R91 (*22*), suggesting a similar disruption of the flavin binding site occurs in many of the R91 variants. Although naturally occurring mutations affecting this residue have not been reported to date, we predict that if discovered, they would give rise to the type II form of methemoglobinemia.

REFERENCES

1. Spatz, L., and Strittmatter, P. (1973) *J. Biol. Chem. 248*, 793−799.
2. Passon, P. G., and Hultquist, D. E. (1972) *Biochim. Biophys. Acta. 275*, 62−66.
3. Keyes, S. R., and Cinti, D. L. (1980) *J. Biol. Chem. 255*, 11357−11364.
4. Oshino, N., Imai, Y., and Sato, R. (1971) *J. Biochem. 69*, 155−167.
5. Hildebrant, A., and Estabrook, R. W. (1971) *Arch. Biochem. Biophys. 143*, 66−79.
6. Reddy, V. V. R., Kupfer, D., and Capsi, E. (1977) *J. Biol. Chem. 252*, 2797−2801.
7. Oshino, N. (1980) in *Hepatic Cytochrome P450 Monooxygenase System* (Schenkman, J. B., and Kupfer, D., Eds.) pp 407−447, Pergamon Press, New York.
8. Paltauf, F., Prough, R. A., Masters, B. S. S., and Johnson, J. M. (1974) *J. Biol. Chem. 249*, 2661−2662.
9. Pugh, E. L., and Kates, M. (1977) *J. Biol. Chem. 252*, 68−73.
10. Fukushima, H., Grinstead, G. F., and Gaylor, J. L. (1981) *J. Biol. Chem. 256*, 4822−4826.
11. Strittmatter, P., Machuga, E. T., and Roth, G. J. (1982) *J. Biol. Chem. 257*, 11883−11886.
12. Loughran, P. A., Roman, L. J., Miller, R. T., and Master, B. S. S. (2001) *Arch. Biochem. Biophys. 385*, 311−321.
13. Kitao, T., Sugita, Y., Yoneyama, Y., and Hattori, K. (1974) *Blood 44*, 879−884.
14. Jaffe, E. R., and Hultquist, D. E. (2001) in *Metabolic and Molecular Basis of Inherited Disease* (Scriver, C. R., Beaudet, A. L., Sly, W. S., and Valle, D., Eds.) 8th ed., Vol. III, pp 4555−4570.
15. Gibson, Q. H. (1948) *Biochem. J. 42*, 13−23.
16. Dekker, J., Eppink, M. H. M., van Dwieten, R., de Rijk, T., Remacha, A. F., Law, L. K., Li, A. M., Cheung, K. L., Berkel, J. H., and Roos, D. (2001) *Blood 97*, 1106−1114.
17. Aalfs, C. M., Salieb-Beugelaar, G. B., Wanders, R. J., Mannens, M. M., and Wijburg, F. A. (2000) *Hum. Mutat. 16*, 18−22.
18. Scott, E. M., and Griffith, I. V. (1959) *Biochim. Biophys. Acta 34*, 584.
19. Leroux, A., Junien, C., Kaplan, J., and Bamberger, J. (1975) *Nature 258*, 619−620.
20. Kobayashi, Y., Fukumaki, Y., Yubisui, T., Inoue, J., and Sakaki, Y. (1990) *Blood 75*, 1408−1413.
21. Yubisui, T., Shirabe, K., Takeshita, M., Kobayashi, Y., Fukumaki, Y., Sakaki, Y., and Takano, T. (1991) *J. Biol. Chem. 266*, 66−70.
22. Marohnic, C. C., and Barber, M. J. (2001) *Arch. Biochem. Biophys. 389*, 223−233.
23. Beck-von Bodman, S. B., Schuler, M. A., Jollie, D. R., and Sligar, S. G. (1986) *Proc. Natl. Acad. Sci. U.S.A. 83*, 9443−9447.
24. Davis, C. A., Dhawan, I. K., Johnson, J. L., and Barber, M. J. (2002) *Arch. Biochem. Biophys. 400*, 63−75.
25. Barber, M. J., Desai, S. K., Marohnic, C. C., Hernandez, H. H., and Pollock, V. V. (2002) *Arch. Biochem. Biophys. 402*, 38−50.
26. Bewley, M. C., Marohnic, C. C., and Barber, M. J. (2001) *Biochemistry 40*, 13574−13582.
27. Matthews, B. W. (1968) *J. Mol. Biol. 33*, 491−497.
28. Collaborative Computational Project No. 4 (1991) *Amore, A Suite of Programs for Protein Crystallography*, Warrington Laboratory, Daresbury, U.K.
29. Brunger, A. T., Adams, P. D., Clore, G. M., DeLano, W. L., Gros, P., Grosse-Kunstleve, R. W., Jiang, J. S., Kuszewski, J., Nilges, M., Pannu, N. S., Read, R. J., Rice, L. M., Simonson, T., and Warren, G. L. (1998) *Acta Crystallogr. D54*, 905−921.
30. Strittmatter, P., Kittler, J. M., Coghill, J. E., and Ozols, J. (1992) *J. Biol. Chem. 267*, 2519−2523.
31. Correll, C. C., Ludwig, M. L., Bruns, C. M., and Karplus, P. A. (1993) *Protein Sci. 2*, 2112−2133.
32. Loverde, A., and Strittmatter, P. (1968) *J. Biol. Chem. 243*, 5779−5787.
33. Strittmatter, P., Kittler, J. M., and Coghill, J. E. (1992) *J. Biol. Chem. 267*, 20164−20167.
34. Hackett, C. S., Novoa, W. B., Kensil, C. R., and Strittmatter, P. (1988) *J. Biol. Chem. 263*, 7539−7543.
35. Sun, M., Moore, T. A., and Song, P. S. (1972) *J. Am. Chem. Soc. 94*, 1730−1740.
36. Edmondson, D. E., and Tollin, G. (1971) *Biochemistry 10*, 113−124.
37. Dwyer, T. M., Mortl, S., Kemter, K., Bacher, A., Fauq, A., and Frerman, F. E. (1999) *Biochemistry 38*, 9735−9745.
38. Kimura, S., Nishida, H., and Iyanagi, T. (2001) *J. Biochem. 130*, 481−490.
39. Strittmatter, P. (1959) *J. Biol. Chem. 234*, 2665−2669.
40. Esnouf, R. M. (1997) *J. Mol. Graphics Modell. 15*, 132−134.
41. Merritt, E. A., and Bacon, D. J. (1997) *Methods Enzymol. 277*, 505−524.

BI034915C